scientific reports

Check for updates

OPEN

Molecular dynamics-based computational investigations on the influence of tumor suppressor p53 binding protein against other proteins/peptides

Mohnad Abdalla[1]✉, Sozan M. Abdelkhalig[2], Uwem O. Edet[3]✉, James H. Zothantluanga[4], Ekementeabasi Aniebo Umoh[5], Ehssan Moglad[6], Nkoyo Ani Nkang[7], Meshari M. Hader[8], Tariq Mohammed R. Alanazi[9], Sawsan AlShouli[10] & Samia Al-Shouli[11]

The tumor-suppressing p-53 binding protein is a crucial protein that is involved in the prevention of cancer via its regulatory effect on a number of cellular processes. Recent evidence indicates that it interacts with a number of other proteins involved in cancer in ways that are not fully understood. An understanding of such interactions could provide insights into novel ways p53 further exerts its tumour prevention role via its interactions with diverse proteins. Thus, this study aimed to examine the interactions of the p53 protein with other proteins (peptides and histones) using molecular simulation dynamics. We opted for a total of seven proteins, namely 2LVM, 2MWO, 2MWP, 4CRI, 4 × 34, 5Z78, and 6MYO (control), and had their PBD files retrieved from the protein database. These proteins were then docked against the p-53 protein and the resulting interactions were examined using molecular docking simulations run at 500 ns. The result of the interactions revealed the utilisation of various amino acids in the process. The peptide that interacted with the highest number of amino acids was 5Z78 and these were Lys10, Gly21, Trp24, Pro105, His106, and Arg107, indicating a stronger interaction. The RMSD and RMSF values indicate that the complexes formed were stable, with 4CRI, 6MYO, and 2G3R giving the most stable values (less than 2.5 Å). Other parameters, including the SASA, Rg, and number of hydrogen bonds, all indicated the formation of fairly stable complexes. Our study indicates that overall, the interactions of 53BP1 with p53K370me2, p53K382me2, methylated K810 Rb, p53K381acK382me2, and tudor-interacting repair regulator protein indicated interactions that were not as strong as those with the histone protein. Thus, it could be that P53 may mediate its tumour suppressing effect via interactions with amino acids and histone.

Keywords Cancer, Simulation, In-silico, p53 protein, Peptides, Prevention

The tumour-suppressing p53-binding protein is a pivotal protein that plays a crucial role in preventing tumourigenesis, primarily through its transcriptional regulation of a network of target genes that mediate various cellular processes[1,2]. Originally recognised for its critical regulation in response to acute DNA damage, recent

[1]Pediatric Research Institute, Children's Hospital Affiliated to Shandong University, Jinan, China. [2]Department of Basic Medical Sciences, College of Medicine, AlMaarefa University, P.O. Box 71666, Riyadh 11597, Saudi Arabia. [3]Department of Biological (Microbiology), Faculty of Natural and Applied Sciences, Arthur Jarvis University, Akpabuyo, Cross River State, Nigeria. [4]Department of Pharmaceutical Sciences, Faculty of Science and Engineering, Dibrugarh University, Dibrugarh 786004, Assam, India. [5]Department of Human Physiology, Faculty of Basic Medical Sciences, Arthur Jarvis University, Akpabuyo, Cross River State, Nigeria. [6]Department of Pharmaceutics, College of Pharmacy, Prince Sattam bin Abdulaziz University, P.O. Box 173, Alkharj 11942, Saudi Arabia. [7]Science Laboratory Department, Faculty of Biological Sciences, University of Calabar, Calabar, Cross River State, Nigeria. [8]Dietary Department, Dr. Soliman Fakeeh Hospital, Jeddah, Saudi Arabia. [9]Security Forces Hospital, Riyadh, Saudi Arabia. [10]Pharmacy Department, Security Forces Hospital, Riyadh 11481, Saudi Arabia. [11]Immunology Unit, Department of Pathology, College of Medicine, King Saud University, Riyadh 11461, Saudi Arabia. ✉email: mohnadabdalla200@gmail.com; uwemedet27@gmail.com

studies have unveiled new pathways through which it exercises its tumour-suppressing function[1,3]. The activity of p53 is chiefly restrained by the ubiquitin E3 ligase Mdm2, although the detailed regulation of the Mdm2-p53 pathway is not entirely understood. In particular research, the RNA binding protein RALY has been identified as an oncogenic factor in lung cancer, highlighting a level of complexity in the regulation and activity of p53 in tumour prevention[4] As a sequence-specific DNA-binding protein, p53 regulates the transcription of downstream targets involved in cell cycle progression, apoptosis, senescence, cell metabolism, and DNA damage repair. The disordered C-terminal domain of p53 controls its transcriptional activities, hinting at the structural intricacies governing its function[5]. The p53 protein is noted for its mutation in about half of all cancers[6], with its signalling network being perturbed in nearly all cancers[5]. Through its selective activation of genes in response to different stress stimuli, p53 orchestrates a cellular response that could either promote survival or trigger cell death. This decision-making ability of p53 between life and death responses to cellular stressors remains a significant area of research, illustrating its pivotal role in cancer biology[7]. Despite the recognised importance of p53 transcriptional activation in these responses, the precise mechanisms underlying its tumour suppression function have been elusive. Notably, no single or compound mouse knockout of specific p53 target genes has replicated the dramatic tumour predisposition, reflecting the critical and complex role of p53 in tumour suppression[8].

Biologically, 53BP1's role in DNA damage response is well known, and this role is carried out via its ability to specifically recognise post-translational modification of histones such as the H4K20me2, a process that allows for the recruitment of 53BP1 to the damage site and triggering of either the homologous recombination (HR) or non-homologous end joining (NHEJ) pathways[9,10]. The balance between both pathways is critical for ensuring not just genome stability but preventing tumorigenesis[9,10]. Furthermore, experimental evidence indicates that there is an interplay between various histone modifications in 53BP1's role in DNA damage repair[9,11]. For instance, it has been shown that the state of methylation at lysine 20 (H4K20) has the capacity to influence 53BP's ability to bind chromatin and effect repair to DNA (Carr et al., 2014). In another study, the acetylation of H4K16 seems to limit 53BP1's chromatin association, thus favouring homologous recombinant[11]. Put together, available experimental evidence seems to indicate that certain modifications affect the recruitment ability of the 53BP1 and vis-a-vis its DNA repair function.

Several proteins with respective pathways linked to cancer therapy exist, and these include histones, tudor interacting repair regulating proteins, and many others[9,10]. One notable protein that plays a vital role in ameliorating cancer is histone[9,10]. Certain research has shown that histone post translational modification has been linked to DNA repairs, maintenance of repressive chromatins and transcription. Modifications of histone have proven efficacy in cancer therapy via diverse pathways[12]. We hypothesise that various histones as well as peptide modifications not only influence 53BP1's role differently but also have clinical relevance in cancer therapy. In previous studies, it has been shown that histone modifications play a crucial role in responding to PARP inhibitors, and DNA-damaging agents[13,14]. Furthermore, an understanding of the mechanisms with which 53BP1 recruitment works as it interacts with diverse proteins could offer novel insights for discovering cancer therapies and enhancing the effectiveness of existing therapies.

Furthermore, interactions of p53 with other proteins, such as histones, can provide clarity on the signalling pathway through which it mediates its role in cancer prevention via in silico approaches. Numerous in-silico approaches to drug discovery has emerged in the last few decades[15]. Collectively, these techniques are called computer-aided drug design. They broadly include the structure-based design, ligand-based design, d*e novo* and fragment-based design, hierarchical virtual screening, MM-GBSA, density functional theory, etc[15]. Practically, these have been applied in various studies to infer lead compounds[16–19]. An understanding of these interactions could help identify prospective target agents for a potential therapy for the management of cancer. Thus, our study was aimed at an understanding of how various histones and peptides interacts with the 53BP1 protein.

Methods

Selection of the study protein

The proteins and their PDB files were obtained from literature and from the protein database, respectively. The proteins were 2LVM[20], 2MWO, 2MWP[21], 4CRI[9], 4×34[22], 5Z78[23], 6MYO[24] and 53BP1[10]. These protein were selected for a couple of reasons. First, they were crystallised and available on the database. Second, these proteins represent a wide range of diverse modifications (acetylation and methylation) p53 can undergoing. Specifically, 2LVM, 2MWO, 2MWP have been implicated in 53BP1 and p53 interactions. Proteins 4×34 and 5Z78 were selected based on their functional implications with the p53 protein. On the other hand, 4CRI and 6MYO were selected as they reflect the diverse post translation modifications such as acetylation, phosphorylation, methylation, and as a control, respectively. Collectively, these proteins were selected based on their biological relevance to cancer biology. Overall, the selection was motivated by the goal of understanding the molecular basis of p53 regulation and the consequences of its modifications in the context of cellular responses to stress and tumour suppression. This rationale is supported by the documented roles of these proteins in the literature and their structural data available in the Protein Data Bank.

Molecular simulation (MS)

Following retrieval of the selected proteins, MS was performed as previously reported using the Desmond tool with all parameters set at default. Our choice of the desmond tool was it is best suited for large complexes like the 53BP1-peptide system and allows for longer runs of up to 500 ns[25]. Furthermore, it has been used in various studies where the MS gave promising results[26,27]. To make results even better we have extended the simulation to 500 ns. To achieve solvation of the proteins, the Desmond building tool and the TIP3P model were utilized. To neutralise the simulation system, a sodium chloride (NaCl) concentration of 0.15 M was used while the temperature and pressure were set at 310k and 1.013 bar[28]. The boundary for the simulation was set at 10 Å orthorhombic box, while the force field utilised was the optimised potential for liquid simulation.

The simulation was performed for 500 ns and the results visualised and analysed using the Desmond virtual molecular operating environment (DVMOE)[29] and as well as Pymol.

Results

Interaction of the tumor suppressor p53 binding protein with other proteins

The crystal structure of the tumour suppressor p53 binding protein 1 (53BP1) is displayed in Fig. 1A, while Table 1 shows the various amino acids involved in the various interactions. The results of the protein-protein interactions between 53BP1 and histone H4K20me2 peptide is given in Fig. 1B. The interacting amino acid residues of 53BP1 is displayed in green colour while that of the histone H4K20me2 peptide is displayed in light blue colour. The amino acids of 53BP1 interacted with a total of 7 amino acids of the histone H4K20me2 peptide such as Lys16, Arg17, His18, Arg19, methyl lysine (Mly)20, Leu22, and Arg23. The results of the protein-protein interactions between 53BP1 and p53K370me2 peptide is given in Fig. 1C. The interacting amino acid residues of 53BP1 is displayed in green colour while that of the p53K370me2 peptide is displayed in purple colour. The amino acids of 53BP1 interacted with a total of 6 amino acids of the p53K370me2 peptide such as His365, His368, Mly370, Ser371, Gln375, and THr377. The 6MYO is a mutation of 53BP1 in two positions Fig. 1H.

Furthermore, the results of the protein-protein interactions between 53BP1 and p53K382me2 peptide is given in Fig. 1D. The interacting amino acid residues of 53BP1 are displayed in green colour while those of the p53K382me2 peptide are displayed in yellow colour. The amino acids of 53BP1 interacted with a total of 4 amino acids of the p53K382me2 peptide such as Ser378, Arg379, His380, and Mly382. On the other hand, the results

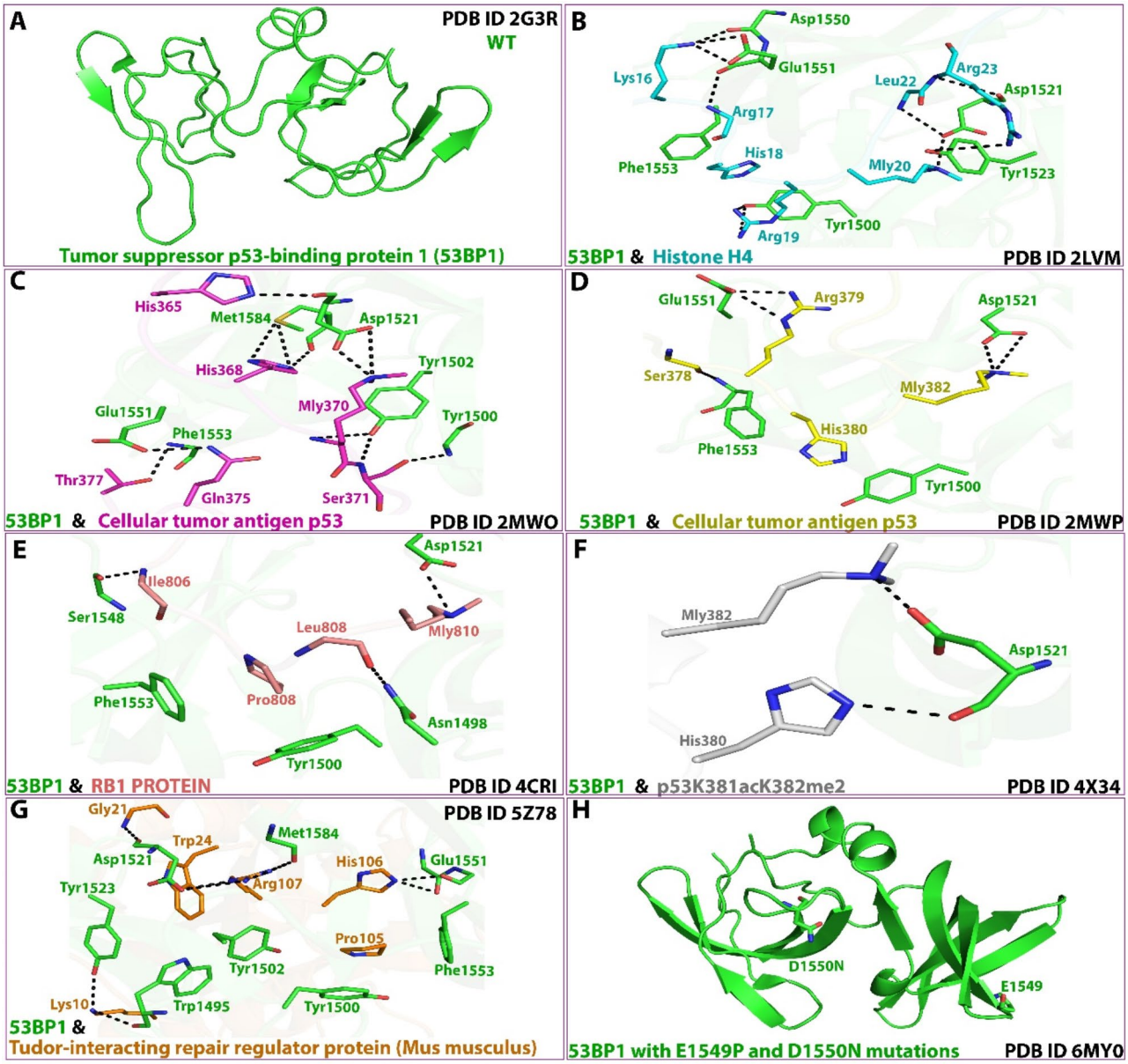

Fig. 1. Interactions of the 53BP1 (**H**) and other proteins (**A**–**G**).

	2G3R	2LVM	2MWO	2MWP	4CRI	4×34	5Z78	6MY0
Trp1495							*	
Asn1498					*			
Tyr1500		*	*	*	*		*	
Tyr1502			*				*	
Asp1521		*	*	*	*	*	*	
Tyr1523		*					*	
Ser1548					*			
Asp1550		*						
Glu1551		*	*	*			*	
Phe1553		*	*	*	*		*	
Met1584			*				*	

Table 1. The amnio acids from 53BP1involved in the interaction.

of the protein-protein interactions between 53BP1 and methylated K810 Rb peptide is given in Fig. 1E. The interacting amino acid residues of 53BP1 are displayed in green colour while those of the methylated K810 Rb peptide is displayed in light pink colour. The amino acids of 53BP1 interacted with a total of 4 amino acids of the methylated K810 Rb peptide such as Ile806, Pro808, Leu808, and Mly810.

The results of the protein-protein interactions between 53BP1 and the p53K381acK382me2 peptide is given in Fig. 1F. The interacting amino acid residues of 53BP1 are displayed in green color while those of the p53K381acK382me2 peptide are displayed in silver colour. The amino acids of 53BP1 interacted with a total of 2 amino acids of the p53K381acK382me2 peptide, such as His380 and Mly382. The results of the protein-protein interactions between 53BP1 and tudor-interacting repair regulator protein are given in Fig. 1G. The interacting amino acid residues of 53BP1 are displayed in green colour while that of the tudor-interacting repair regulator protein is displayed in orange colour. The amino acids of 53BP1 interacted with a total of 6 amino acids of the tudor-interacting repair regulator proteins such as Lys10, Gly21, Trp24, Pro105, His106, and Arg107.

As shown in Table 1 and 53BP1 interacted differently with the various proteins using different numbers of amino acids. The amino acids involved in the various interactions were Trp1495, Asn1498, Tyr1500. Tyr1502, Ser1548, Asp1550, Glu1551, Phe1553, and Met1584. Proteins 2G3R and 6MY0 did not return any interacting amino acid as shown Table 1; Fig. 1. However, for 2G3R and 2MWO, the number of amino acids were 6 while for 2MWP, 4 amino acids were involved in the interaction, while for 4CRI and 4×34, the amino acids involved were 5 and 1, respectively, while 5Z78 returned the highest number of interacting amino acids with 7 amino acids.

MS data of the interactions

In addition to the evaluation of the various interactions in terms of interacting amino acids, the various interactions were also evaluated in terms of their stability using molecular simulation parameters such as RMSD, RMSF, SASA, Rg, and number of hydrogen bonds. The RMSD, that is, the root mean square deviation of the atomic position result is presented in Figs. 2A, 3 and 4. Figure 2A shows the result, of the simulation run for 500 ns, and overall, it indicates variations in the RMSD values. The RMSD values of 4CRI, 6MYO, and 2G3R returned the least values that were generally less than 2.5 Å during their interactions with the p53 protein, while the rest (2LVM, 5Z78, 2MWP, 4×34, and 2MWO) returned values that were well over ranged from > 2 to 6 Å during the entire 500 ns run. Specifically, 3G3R gave the least RMSD that was less than 2.5 Å during the entire simulation duration. Similarly, 6MYO gave RMSD values that were were within 1–2.5 Å. The RMSD value for 4CRI, for the first 400 ns was below 2.5 Å, while between 400 and 500 ns, the RMSD value was 3–5.75 Å. On the other, 2LVM, 5Z78, 2MWP, 4×34 and 2MWO, the values were higher than 2 Å. The RMSD values for 2LVM, 5Z78, 2MWP, and 4×34 ranged from > 2–5 Å, while for 2MWO, it ranged from 3.5 to 6 Å. As a parameter, RMSD value is used as a measure of the differences usually observed between proteins during simulation runs. By returning the least RMSD values, 4CRI, 6MYO, and 2G3R were the most stable, implying that they gave the best or most stable complexes.

In addition to the RMSD, RMSF values were evaluated for the various proteins. To make the values more clearer, these were separated into two (Fig. 2B,C). Consistently, all the proteins showed variations in RMSF values. Overall, 5Z78 showed the highest number of spikes that were above 2.5 Å. Consistently, all the proteins gave RMSF values that were above 2 Å at amino acid residues 375, 1480, 1490–1500, 1550, 1560, and 1570–1580. However, at amino acid residue 1600, only 5Z78 gave an RMSF value that was higher than 2 Å (Fig. 2B). At lower amino acid residues, 5Z78 also gave higher RMSF values, especially at residues less than 200, while 2MWO, and 2MWP gave RMSF values that were higher than 2 Å.

Figure 2D shows the result for the SASA values for the various complexes. The result indicates that the complexes, apart from 5Z78 that gave SASA value that was consistent around 18,000 nm^2 for the simulation duration. Consistently, for other proteins, their SASA values were between 7000 and 9000 nm^2 for the entire simulation runs. In addition to the SASA value, the radius of gyration Rg is presented in Fig. 2E for the complexes as a plot of radius and the simulation run time. The Rg values for 5Z78 were the highest and consistent at 25 nm^2. On the other hand, the rest of the other proteins gave Rg values that ranged from 12.5 to 16.0 nm^2. Figure 2F shows the number of hydrogen bonds in the various complexes during the simulation run. The result indicates

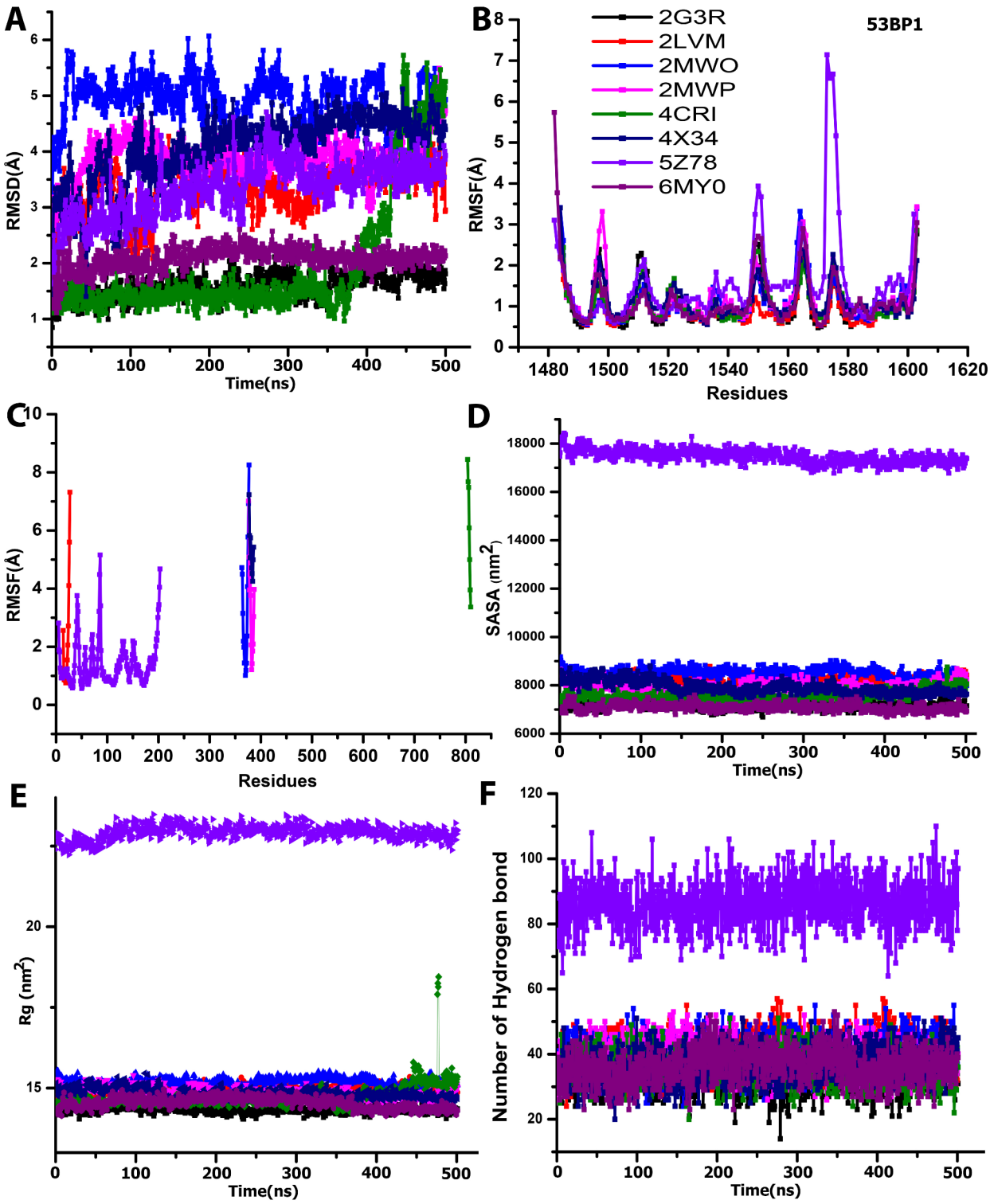

Fig. 2. A comparison of RMSD, RMSF, SASA Rg, and number of hydrogen bonds.

that 5Z78 gave the highest number of hydrogen bonds that ranged from 65 to 110, while others gave hydrogen bonds that ranged from 10 to 50. throughout the simulation run.

Figure 3 shows a validation of the RMSD from the VDM and Desmond using Pymol and this was done using three point validations (0, 250 and 500 ns) to achieve a clearer of the structure and the RMSD values and the structures very clearly. Figure 4 shows the heatmap of the RMSD values of the various complexes. The findings in the heatmap corroborates the RMSD in Fig. 2A, and it indicates that 2MWO had the highest RMSD further conforming it formed the most unstable complex.

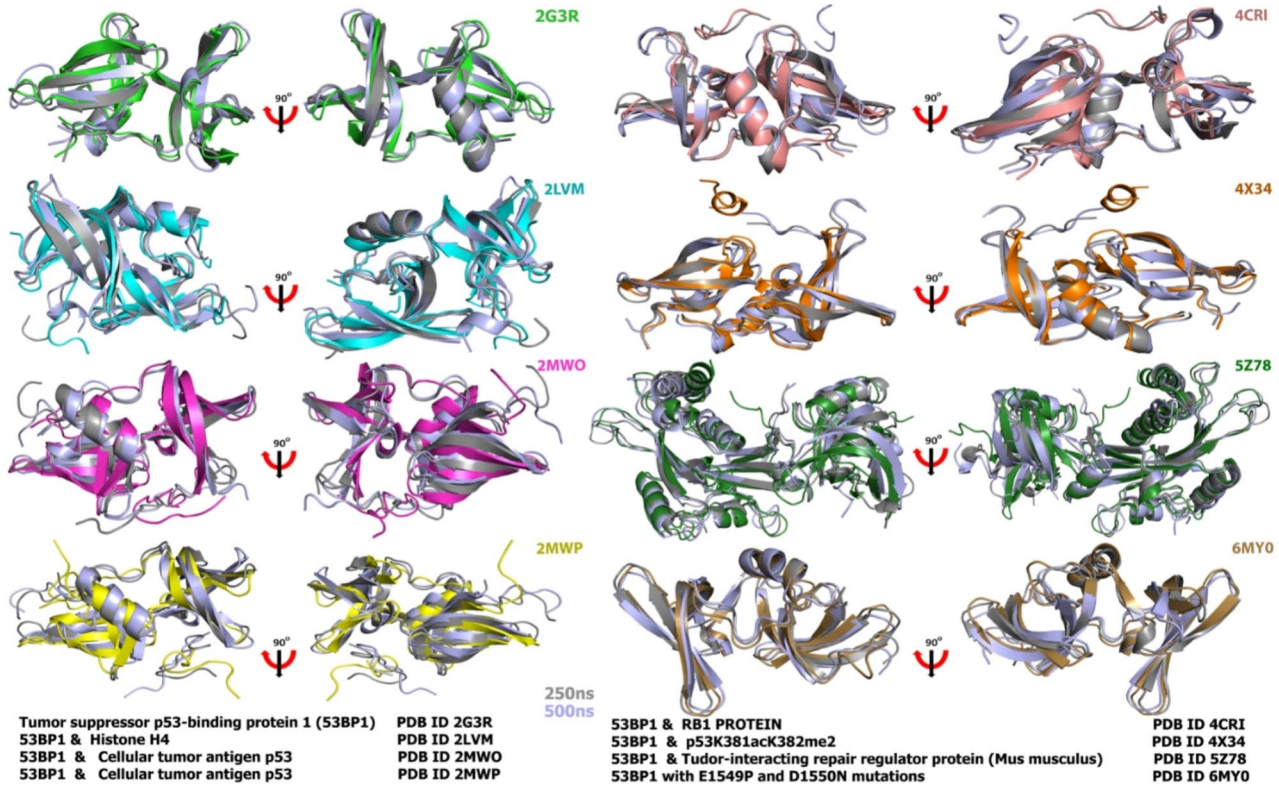

Fig. 3. Structure superimposed for RMSD at 250 and 500 ns for complexes tumor suppressor p53-binding protein 1 and its interactions with the various proteins used in the study.

Discussion

It is well known that p53 interacts with histones via various routes or modifications that collectively drive the stability, localization, and transcriptional activity of p53[2]. Away from its its interactions with histones, amino acids of the p53 protein can undergone post-translational modifications such as phosphorylation, methylation, and ubiquitination. These modifications are critical in the protein's response to DNA damage, enhancing p53's affinity for DNA and promoting its transcriptional activity[30,31]. These interactions have been implicated in cancer therapy, and this informed study. In our study, we sought to understand the interactions of diverse proteins as they interact the p53-binding protein 1.

Our findings indicate the involvement of diverse amino acids as they interact with the p53-binding protein 1. The involvement of various amino acids in the interaction of the p53 protein is in line with previous reports that also showed that p53 and other complex proteins such as SARS-Cov1 or 2 proteins are capable of interaction with other human or animal derived proteins in various ways[28,29,32,33]. The number of amino acids involved in the interaction is an indication of the strength of the interactions. This implies that the interaction between 2G3R and 5Z78 that gave the highest number of amino acids ($n=7$) gave the strongest interaction. The 2G3R protein is a protein whose most important chain is the A chain with an amino acid chain length of 120 that plays an important role in cancer[3]. The amino acids involved in the interaction with the histone H4K20me2 peptide were Lys16, Arg17, His18, Arg19, Mly20, Leu22, and Arg23. In the 5Z78 structure, we observed 53BP1 residues W1495, Y1523, D1521, Y1502, and F1519 undergoes conformational changes upon TIRR interaction. In particular, residues W1495 and Y1523 display the largest conformational change and completely alter the structure of the aromatic cage.

Some amino acid residues were observed to be involved in the strongest interactions, and these were Lys10, Gly21, and Trp24. As a residue, Lys10 is a significant amino acid due to its ammonium group as it can form salt bridges with the negatively charged residues in the 53BP1 TTD, contributing to a stable interaction. The presence of lysine residues has been shown to contribute to the overall stability of interactions of complexes in microorganisms[34]. In our study, electrostatics interaction could enhance the stability of the complexes as well as the specificity and affinity of binding as p53 binds with co-factors during DNA damage repair. As further noted, the Lys10 residue was conserved across other proteins that interacted with the p35. This could suggest a common mechanism of action where charged residues drive stability and binding via electrostatic interactions that is key to DNA damage repair. As an amino acid, glycine possesses small side chains as part of its structure, and they are known to provide proteins with flexibility[35]. In this context, the presence of Gly 21 residue could facilitate conformations in p53 that can promote stability of the complexes during DNA damage repair and other roles played by p53. Our assertion is in line with a recent report that showed that severe or prolonged starvation of cells with serine/glycine or glutamine would induce DNA damage[2], further confirming their role in

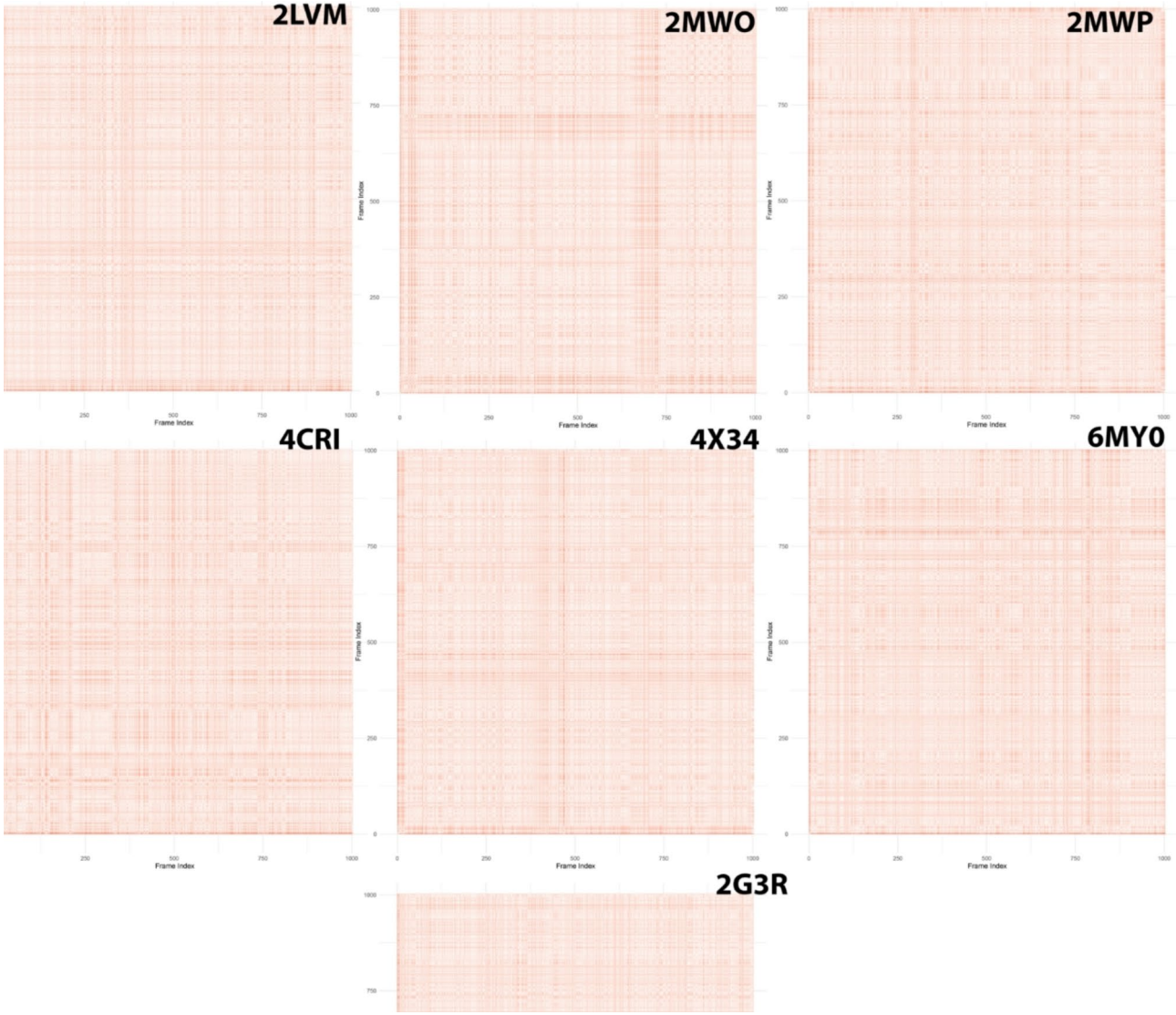

Fig. 4. Heatmap of calculated RMSD values from the original crystal file for the various formed complexes.

maintaining the integrity of DNA structure. Furthermore, another amino acid involved in the strong interaction was Trp24. As an amino acid, tryptophan possesses an aromatic ring with which it interacts with other residues using hydrophobic interactions and π-π stacking with other aromatic residues in the binding pocket of 53BP1, and in the process helps to stabilise functional conformation of p53. Put together, Lys10, Gly21, and Trp24 residues could be involved in maintaining the stability and flexibility of the complexes formed with p53 when recruited to the site of DNA damage, thus enhancing its tumour suppression property. Their conservation across all the proteins that interacted with the p53 protein indicates the role of evolution in the prevention of cancer.

In addition, in non-small cell lung cancer, histone has been shown to be a promising target site for suppressing growth of tumour cells via its G9a, a lysine methyltransferase belonging to the Su (Var) 3–9 family[36]. This effect was mediated through the Wnt signalling pathway, an ancient and evolutionarily conserved pathway that regulates crucial aspects of cell fate determination, cell migration, polarity, neural patterning, and organogenesis during embryonic development. It was also shown that this effect was possible via down-regulation of heterochromatin protein − 1α (HP-1α). The interaction between p53 binding proteins with histone shows more binding affinity with Lys16, Arg17, His18, Arg19, Mly20, Leu22, and Arg23. It has also been established that histone H4 lysine 16 acetylation (H4K16Ac) and its acetyltransferase hMOF are linked to the regulation of TMS1/ASC, a proapoptotic gene that undergoes epigenetic silencing in human cancers. The research further suggested that the selective marking of nucleosomes flanking the CpG island by histone acetyltransferase hMOF is essential in maintaining TMS1 activity of the gene. Therefore, the loss of H4K16Ac, mobilisation of nucleosomes, and transcriptional down regulation may be important events in the epigenetic silencing of certain tumour suppressor genes in cancer[37].

Furthermore, arginine has also been linked as a signalling molecule, an epigenetic regulator, and a mitochondrial modulator in cancer cells. It is more associated as a cancer causative than a therapy. Hence,

deprivation of arginine is considered a cancer therapy[38]. Also, histidine or His 18 is seen to play an essential role as a cancer therapy. The combination of exogenous histidine with sorafenib (Nexavar @), the only currently approved anti-cancer drug for patients with advanced hepatocellular carcinoma (HCC) enhanced the treatment of the latter cancer by reducing the tumour cells in the treated subject, hence making the use of sorafenib (Nexavar @) effective[39]. Leucine, on the other hand, has been linked to the promotion of tumour cells. A certain research has shown that leucine supplementation enhances tumour growth in both lean and overweight mice, further accelerating pancreatic cancer in the mice[40]. Subsequent interaction of 53BP1 with p53K370me2, p53K382me2, methylated K810 Rb, p53K381acK382me2, and tudor-interacting repair regulator protein showed limited reaction with proteins or amino acids compared to that of Histone. Irrespective of the fact that the reactions between various amino acids as seen between 53BP1 and histones were with some who had tendencies to enhance tumour growth, a greater percentage were actually indicated in suppressing tumour cells and enhancing the treatment efficacy of cancer. Therefore, the p53 binding protein mediates its tumour-suppressing effect by binding histone and activating amino acids of the pathway. Signalling pathways associated with histone include the Wnt signalling pathway. Hence, p53 will likely be affiliated with regulation of the said pathway in mediating its tumour suppressing effect.

The dimethylation of lysine 382 (p53K382me2) play a key role in p53's interaction with histone proteins, particularly with the the tandem Tudor domain (TTD) of the 53BP1 protein[21,22]. Other routes by which it mediates its tumor-suppressing effect is through interactions with histone proteins and amino acids include modification recognition of histones such as the methylated histone H4K20me[10] and via acetylation and transcriptional activation[41,42]. Acetylation of key residues such as lysine residues like K381 and K382 enhances the transcriptional activity[41,42]. It is also known that the interplay between methylation and acetylation determines p53's tumor-suppressive role[26]. Another pathway is via histone reading proteins that include those within the Tudor domain have the capacity to recognise specific methylated states of p53 and histones, and in the process facilitate DNA repair[43,44]. In 5Z78 structure, we observed 53BP1 residues W1495, Y1523, D1521, Y1502, and F1519, undergoes conformational changes upon TIRR interaction. In particular, residues W1495 and Y1523 display the largest conformational change and completely alter the structure of the aromatic cage.

As a protein p53 is prone to mutations whose accumulations give rise to cancer[6]. These mutations exert their negative effects via a number of ways that include loss of ability to bind with co-factors and altered conformational dynamics[21,22], preventing of appropriate post translation modifications[45,46]. The strong interaction observed in our study by several amino acids in all the protein indicate an absence of mutation effect on the interactions. Thus, in addition n addition to the interacting amino acids, other simulation parameters were also evaluated, and these were RMSD, RMSF, SASA, and Rg. Ideally, the RMSD value for a complex should be zero where it indicates absolute resemblance of the complex to the reference complex. However, practically, it is not possible to attain this in practice due to statistics[47,48]. As a parameter, it provides insight into the stability and function of a protein[47,49]. However, an RMSD values of 2.5 Å and less indicate stability, while higher values suggest complexes that are not stable and far from the control. Thus, this indicates that 2G3R was more stable than the control complex 6MYO, while 4CRI was also stable for the most of the run. Furthermore, higher RMSD values indicate dissimilarities or an unstable complex, while low RMSD values as returned by 4CRI, 6MYO and 2G3R indicate stable complexes[33]. As a parameter, the RMSF is a measure of the flexibility of each residue and their movement over the simulation run, and it is related to the function of the protein. It is used to evaluate which of the residues were responsible for the structural motion of the protein48 As a rule of thumb, RMSF values are less the 2 Å for two proteins indicate that they closely resemble each other. In our study, 5Z78, 2MWO, and 2MWP gave values that were not close to the control, 6MYO, indicating that they had more residues that were driving the structural motion of the protein[47]. Our result further indicates that all the proteins apart from 5Z78 and 2MWP, gave lower RMSF values, suggesting that they are stable. Those with higher RMSF indicate that the complexes formed were not stable, and this could be due to conformational changes to the protein as a result of mutations. In an earlier study that utilised simulation dynamics of the full-length p53 monomer[50]. In their study, it was noted that the RMSF values of the amino residues between 100 and 300 ns gave the least values and conformed to our findings. This region is known as the DNA binding region and the low RMSF values indicates stable complexes for all the complexes. Stability in this region indicates limited conformation changes and is linked to effective binding of DNA[51]. In another study designed to evaluate the inhibitory properties of 100B ligand to block S100B–p53 interaction, it was noted that the RMSD values of the formed complexes revealed regions of stability (low RMSD) and flexibility (high RMSD values)[52]. Balasundaram & Doss[53] in their study observed higher deviations in RMSD and RMSF values for the mutant p53 protein compared to the native one.

As a parameter, it is used to measure the surface of a protein that is accessible to a solvent[54]). The SASA value of a protein or complex is an important factor that is taken into consideration when it comes to folding and stability of a protein in addition to other desirable properties such as thermodynamics[55]. Our SASA results for the complexes ranged from 7000 to 9000 nm^2 for all the complex except for 5Z78 that was consistently around 18,000 nm^2. This indicates that the later had more solvent area accessible for solvents. This finding aligns with that of an earlier study that reported variation in SASA values[47]. Our reported SASA values were lower than those reported an earlier study that evaluated the interaction of proteins with SARS-COV2. The lowered SASA values is an indication of stability of the complexes[47]. Rg of a complex allows for the assessment of the stability of a protein's[56] Rg is a measure of the root mean square distance of the electrons in a molecule from their centre of gravity, and as a parameter it is used to evaluate the stability of a compound or complex[47]. A low Rg indicates a tightly packed protein, that is, a stable protein, implying that all the complexes were fairly stable. Compared to other parameters evaluated so far, Rg showed the least fluctuation, and an increase in Rg has been linked to increased surface area accessible to a drug or solvent. Our Rg values showed that for all the complexes except for 5Z78 which recorded the largest, their Rg values were within range of the control 6MYO. Overall, the complexes all showed slight fluctuations in their values which indicates that the complexes are exploring

various conformations. Furthermore, the complexes with lower Rg values indicates more compact complexes, suggesting that all the complexes except 5Z78 were as compact as the control. Our complexes were less compact than those of an earlier on Sars-cov2 protein-inhibitor complexes[57].

Conclusion

P53 mediates its tumour suppressing effect via interactions with amino acids and histone. The Wnt signalling pathway is a possible pathway through which it mediates its effect as it is related to Histone. However, p53 may also be associated with other proteins such as p53K370me2, p53K382me2, methylated K810 Rb, p53K381acK382me2, and tudor-interacting repair regulator protein. Though its interactions with the amino acids and other molecules of these proteins are limited compared to those with histones.

Limitation of the study

This study was limited to bioinformatics procedures. In vivo study will also be needed to ascertain the effect of p53 in comparism to the result generated from docking procedures.

Data availability

Data are made available following request from corresponding or first author.

Received: 16 August 2024; Accepted: 27 November 2024
Published online: 02 December 2024

References

1. Hernández Borrero, L. J. & El-Deiry, W. S. Tumor suppressor p53: Biology, signaling pathways, and therapeutic targeting. Biochimica et biophysica acta. *Reviews cancer*. **1876** (1), 188556. https://doi.org/10.1016/j.bbcan.2021.188556 (2021).
2. Lacroix, M., Riscal, R., Arena, G., Linares, L. K. & Le Cam, L. Metabolic functions of the tumor suppressor p53: implications in normal physiology, metabolic disorders, and cancer. *Mol. Metabolism*. **33**, 2–22 (2020).
3. Boutelle, A. M. & Attardi, L. D. p53 and tumor suppression: it takes a network. *Trends Cell Biol.* **31**, 298–310. https://doi.org/10.1016/j.tcb.2020.12.011 (2021).
4. Hu, H. et al. The RNA binding protein RALY suppresses p53 activity and promotes lung tumorigenesis. *Cell. Rep.* **42**, 112288. https://doi.org/10.1016/j.celrep.2023.112288 (2023).
5. Zhang, L. et al. A p53/LINC00324 positive feedback loop suppresses tumor growth by counteracting SET-mediated transcriptional repression. *Cell. Rep.* **42**, 112833. https://doi.org/10.1016/j.celrep.2023.112833 (2023).
6. Rivlin, N., Brosh, R., Oren, M. & Rotter, V. Mutations in the p53 tumor suppressor gene: important milestones at the various steps of Tumorigenesis. *Genes cancer*. **2** (4), 466–474. https://doi.org/10.1177/1947601911408889 (2011).
7. Liu, Y., Leslie, P. L. & Zhang, Y. Life and death decision-making by p53 and implications for Cancer Immunotherapy. *Trends cancer*. **7**, 226–239. https://doi.org/10.1016/j.trecan.2020.10.005 (2021).
8. Bieging, K. T. & Attardi, L. D. Deconstructing p53 transcriptional networks in tumor suppression. *Trends Cell Biol.* **22**, 97–106. https://doi.org/10.1016/j.tcb.2011.10.006 (2012).
9. Carr, S. M. et al. Lysine methylation-dependent binding of 53BP1 to the pRb tumor suppressor. *Proc. Natl. Acad. Sci. U.S.A.* **111**, 11341–11346. https://doi.org/10.1073/pnas.1403737111 (2014).
10. Botuyan, M. V. et al. Structural basis for the methylation state-specific recognition of histone H4-K20 by 53BP1 and Crb2 in DNA repair. *Cell* **127**, 1361–1373. https://doi.org/10.1016/j.cell.2006.10.043 (2006).
11. Feng, L. et al. Acetylation limits 53BP1 association with damaged chromatin to promote homologous recombination. *Nat. Struct. Mol. Biol.* **20** (3), 317–325 (2013).
12. Audia, J. E. & Campbell, R. M. Histone Modifications and Cancer. *Cold Spring Harbor Perspect. Biol.* **8**, a019521. https://doi.org/10.1101/cshperspect.a019521 (2016).
13. Lee, E. K. & Konstantinopoulos, P. A. PARP inhibition and immune modulation: scientific rationale and perspectives for the treatment of gynecologic cancers. *Therapeutic Adv. Med. Oncol.* **12**, 1758835920944116. https://doi.org/10.1177/1758835920944116 (2020).
14. Yang, Y., Zhang, M. & Wang, Y. The roles of histone modifications in tumorigenesis and associated inhibitors in cancer therapy. *J. Natl. Cancer Cent.* **2** (4), 277–290. https://doi.org/10.1016/j.jncc.2022.09.002 (2022).
15. Chang, Y. et al. A guide to. *Silico Drug Des. Pharm.* **15** (1), 49. https://doi.org/10.3390/pharmaceutics15010049 (2022).
16. Gupta, A. & Purohit, R. Identification of potent BRD4-BD1 inhibitors using classical and steered molecular dynamics based free energy analysis. *J. Cell. Biochem.* **125** (3), e30532. https://doi.org/10.1002/jcb.30532 (2024).
17. Singh, R., Manna, S., Nandanwar, H. & Purohit, R. Bioactives from medicinal herb against bedaquiline resistant tuberculosis: removing the dark clouds from the horizon. *Microbes Infect.* **26** (3), 105279. https://doi.org/10.1016/j.micinf.2023.105279 (2024).
18. Singh, R., Bhardwaj, V. K., Sharma, J., Das, P. & Purohit, R. Identification of selective cyclin-dependent kinase 2 inhibitor from the library of pyrrolone-fused benzosuberene compounds: an in silico exploration. *J. Biomol. Struct. Dyn.* **40** (17), 7693–7701. https://doi.org/10.1080/07391102.2021.1900918 (2022).
19. Rajasekaran, R. et al. Effect of deleterious nsSNP on the HER2 receptor based on stability and binding affinity with herceptin: a computational approach. *C.R. Biol.* **331** (6), 409–417. https://doi.org/10.1016/j.crvi.2008.03.004 (2008).
20. Tang, J. et al. Acetylation limits 53BP1 association with damaged chromatin to promote homologous recombination. *Nat. Struct. Mol. Biol.* **20**, 317–325. https://doi.org/10.1038/nsmb.2499 (2013).
21. Tong, Q. et al. Structural plasticity of methyllysine recognition by the tandem tudor domain of 53BP1. *Struct. (London England: 1993)*. **23**, 312–321. https://doi.org/10.1016/j.str.2014.11.013 (2015).
22. Tong, Q. et al. An acetyl-methyl switch drives a conformational change in p53. *Struct. (London England: 1993)*. **23**, 322–331. https://doi.org/10.1016/j.str.2014.12.010 (2015).
23. Dai, Y., Zhang, A., Shan, S., Gong, Z. & Zhou, Z. Structural basis for recognition of 53BP1 tandem Tudor domain by TIRR. *Nat. Commun.* **9**, 2123. https://doi.org/10.1038/s41467-018-04557-2 (2018).
24. Huang, L. S., Lümmen, P. & Berry, E. A. Crystallographic investigation of the ubiquinone binding site of respiratory complex II and its inhibitors. *Biochim. et Biophys. acta Proteins Proteom.* **1869**, 140679. https://doi.org/10.1016/j.bbapap.2021.140679 (2021).
25. Dror, R. O., Dirks, R. M., Grossman, J. P., Xu, H. & Shaw, D. E. Biomolecular Simulation: a computational microscope for Molecular Biology. *Annual Rev. Biophys.* **41** (1), 429–452. https://doi.org/10.1146/annurev-biophys-042910-155245 (2012).
26. Ivanova, L. et al. Molecular dynamics simulations of the interactions between glial cell line- derived neurotrophic factor family receptor GFRα1 and small-molecule ligands. *ACS Omega*. **3** (9), 11407–11414 (2018).
27. Wang, J., Alekseenko, A., Kozakov, D. & Miao, Y. Improved modeling of peptide- protein binding through global docking and accelerated molecular dynamics simulations. *Front. Mol. Biosci.* **6**, 112. https://doi.org/10.3389/fmolb.2019.00112 (2019).

28. Aloufi, A. S. et al. Molecular dynamic analyses of the interaction of SARS-CoV-1 or 2 variants with various angiotensin-converting enzyme-2 species. *J. Biomol. Struct. Dyn.* 1–10. https://doi.org/10.1080/07391102.2024.2314745 (2024).
29. Humphrey, W., Dalke, A. & Schulten, K. VMD: visual molecular dynamics. *J. Mol. Graph.* **14**, 33–38. https://doi.org/10.1016/0263-7855(96)00018-5 (1996).
30. Liu, Y., Tavana, O. & Gu, W. p53 modifications: exquisite decorations of the powerful guardian. *J. Mol. Cell Biol.* **11** (7), 564–577 (2019).
31. Borrero, L. J. H. & El-Deiry, W. S. Tumor suppressor p53: Biology, signaling pathways, and therapeutic targeting. *Biochim. et Biophys. Acta (BBA)-Reviews Cancer*. **1876** (1), 188556 (2021).
32. Ugbe, F. A. et al. Cheminformatics-based discovery of new organoselenium compounds with potential for the treatment of cutaneous and visceral leishmaniasis. *J. Biomol. Struct. Dyn.* 1–24. https://doi.org/10.1080/07391102.2023.2279269 (2023).
33. Nwaokorie, F. et al. In-silico assessment of bioactive compounds from chewing stick (Salvadora Persica) against N-acetylneuraminate lyase (5ZKA) of Fusobacterium nucleatum involved in salicyclic acid metabolism. *J. Mol. Struct.* **1316**, 138733. https://doi.org/10.1016/j.molstruc.2024.138733 (2024).
34. Ahmad, N. N., Kamarudin, A., Leow, N. H., Rahman, R. N. Z. R. A. & A. T. C., & The role of Surface exposed lysine in Conformational Stability and Functional Properties of Lipase from Staphylococcus Family. *Molecules (Basel Switzerland)*. **25** (17), 3858. https://doi.org/10.3390/molecules25173858 (2020).
35. Van Rosmalen, M., Krom, M. & Merkx, M. Tuning the flexibility of glycine-serine linkers to allow rational design of multidomain proteins. *Biochemistry* **56** (50), 6565–6574 (2017).
36. Zhang, K. et al. Targeting histone methyltransferase G9a inhibits growth and wnt signaling pathway by epigenetically regulating HP1α and APC2 gene expression in non-small cell lung cancer. *Mol. Cancer*. **17**. https://doi.org/10.1186/s12943-018-0896-8 (2018).
37. Kapoor-Vazirani, P., Kagey, J. D., Powell, D. R. & Vertino, P. M. Role of hMOF-dependent histone H4 lysine 16 acetylation in the maintenance of TMS1/ASC gene activity. *Cancer Res.* **68**, 6810–6821. https://doi.org/10.1158/0008-5472.can-08-0141 (2008).
38. Chen, C. L., Hsu, S. C., Ann, D. K., Yen, Y. & Kung, H. J. Arginine Signaling and Cancer Metabolism. *Cancers* **13**. https://doi.org/10.3390/cancers13143541 (2021).
39. Park, Y. et al. Impact of Exogenous Treatment with Histidine on Hepatocellular Carcinoma Cells. *Cancers* 14. https://doi.org/10.3390/cancers14051205 (2022).
40. Liu, K. A., Lashinger, L. M., Rasmussen, A. J. & Hursting, S. D. Leucine supplementation differentially enhances pancreatic cancer growth in lean and overweight mice. *Cancer Metabolism*. **2**, 6. https://doi.org/10.1186/2049-3002-2-6 (2014).
41. Luo, J. et al. Acetylation of p53 augments its site-specific DNA binding both in vitro and in vivo. *Proc. Natl. Acad. Sci. U.S.A.* **101** (8), 2259–2264. https://doi.org/10.1073/pnas.0308762101 (2004).
42. Barlev, N. A. et al. Acetylation of p53 activates transcription through recruitment of coactivators/histone acetyltransferases. *Mol. Cell.* **8** (6), 1243–1254. https://doi.org/10.1016/s1097-2765(01)00414-2 (2001).
43. Cui, G. et al. PHF20 is an effector protein of p53 double lysine methylation that stabilizes and activates p53. *Nat. Struct. Mol. Biol.* **19** (9), 916–924. https://doi.org/10.1038/nsmb.2353 (2012).
44. Roy, S. et al. Structural insight into p53 recognition by the 53BP1 tandem Tudor domain. *J. Mol. Biol.* **398** (4), 489–496. https://doi.org/10.1016/j.jmb.2010.03.024 (2010).
45. Kachirskaia, I. et al. Role for 53BP1 Tudor domain recognition of p53 dimethylated at lysine 382 in DNA damage signaling. *J. Biol. Chem.* **283** (50), 34660–34666. https://doi.org/10.1074/jbc.M806020200 (2008).
46. Huang, J. et al. p53 is regulated by the lysine demethylase LSD1. *Nature* **449** (7158), 105–108. https://doi.org/10.1038/nature06092 (2007).
47. Abdalla, M., Eltayb, W. A., El-Arabey, A. A., Singh, K. & Jiang, X. Molecular dynamic study of SARS-CoV-2 with various S protein mutations and their effect on thermodynamic properties. *Comput. Biol. Med.* **141**, 105025 (2022).
48. Arnittali, M., Rissanou, A. N. & Harmandaris, V. Structure of biomolecules through molecular dynamics simulations. *Procedia Comput. Sci.* **156**, 69–78 (2019).
49. Bavi, R., Kumar, R., Choi, L. & Woo Lee, K. Exploration of novel inhibitors for Bruton's tyrosine kinase by 3D QSAR modeling and Molecular Dynamics Simulation. *PloS One*. **11**, e0147190. https://doi.org/10.1371/journal.pone.0147190 (2016).
50. Chillemi, G. et al. Molecular dynamics of the full-length p53 monomer. *Cell. Cycle (Georgetown Tex)*. **12** (18), 3098–3108. https://doi.org/10.4161/cc.26162 (2013).
51. Joerger, A. C. & Fersht, A. R. Structural biology of the tumor suppressor p53. *Annu. Rev. Biochem.* **77**, 557–582. https://doi.org/10.1146/annurev.biochem.77.060806.091238 (2008).
52. Whitlow, J. L., Varughese, J. F., Zhou, Z., Bartolotti, L. J. & Li, Y. Computational screening and design of S100B ligand to block S100B–p53 interaction. *J. Mol. Graph. Model.* **27** (8), 969–977. https://doi.org/10.1016/j.jmgm.2009.02.006 (2009).
53. Balasundaram, A. & Doss, C. G. P. Unraveling the structural changes in the DNA-binding region of tumor protein p53 (TP53) upon hotspot mutation p53 Arg248 by comparative computational approach. *Int. J. Mol. Sci.* **23** (24), 15499 (2022).
54. Shaytan, A. K., Shaitan, K. V. & Khokhlov, A. R. Solvent accessible surface area of amino acid residues in globular proteins: correlation of apparent transfer free energies with experimental hydrophobicity scales. *Biomacromolecules* **10** (5), 1224–1237 (2009).
55. Ali, S. A., Hassan, M. I., Islam, A. & Ahmad, F. A review of methods available to estimate solvent-accessible surface areas of soluble proteins in the folded and unfolded states. *Curr. Protein Pept. Sci.* **15**, 456–476. https://doi.org/10.2174/1389203715666140327114232 (2014).
56. Lobanov, M. Y., Bogatyreva, N. S. & Galzitskaya, O. V. Radius of gyration as an indicator of protein structure compactness. *Mol. Biol.* **42**, 623–628 (2008).
57. Rampogu, S., Lee, G., Park, J. S., Lee, K. W. & Kim, M. O. Molecular Docking and Molecular Dynamics simulations Discover Curcumin Analogue as a plausible dual inhibitor for SARS-CoV–2. *Int. J. Mol. Sci.* **23** (3), 1771. https://doi.org/10.3390/ijms23031771 (2022).

Acknowledgements

We would like to thank AlMaarefa University, Riyadh, Saudi Arabia for supporting this research.

Author contributions

MA, SMA, and UOE conceived the project and ran the analysis. Authors JHZ, EAU, EM, NAN, MMH, TMRA, SA and SA all contributed to and reviewed the final draft.

Declarations

Competing interests

The authors declare no competing interests.

Additional information

Correspondence and requests for materials should be addressed to M.A. or U.O.E.